

Chapter 12

Calcium Sulfate Precipitation Throughout Its Phase Diagram

Alexander E.S. Van Driessche, Tomasz M. Stawski, Liane G. Benning, and Matthias Kellermeier

12.1 Introduction

Over the past decade, significant progress has been made in our understanding of crystallization phenomena. In particular, a number of precursor and intermediate species, both solutes and solids, and either stable or metastable (or even unstable), have been identified. Their existence extends the simplified picture of classical nucleation and growth theories toward much more complex pathways. These newly found species include various solute clusters, liquid-like phases, amorphous particles, and metastable (often nanosized) crystalline polymorphs, all of which may exist for different periods and may convert into one another depending on the chosen conditions (see, for instance, De Yoreo et al. 2017, Chap. 1; Wolf and Gower 2017, Chap. 3; Rodriguez-Blanco et al. 2017, Chap. 5; Birkedal 2017, Chap. 10; Reichel and Faivre 2017, Chap. 14, and references therein). Quite naturally, most

A.E.S. Van Driessche Driessche (✉)
University Grenoble Alpes, CNRS, ISTERre, F-38000 Grenoble, France
e-mail: alexander.van-driessche@univ-grenoble-alpes.fr

T.M. Stawski
German Research Centre for Geosciences, GFZ, D-14473 Potsdam, Germany
School of Earth and Environment, University of Leeds, LS2 9JT Leeds, UK

L.G. Benning
German Research Center for Geosciences, GFZ, Interface Geochemistry Section,
14473 Potsdam, Germany

Department of Earth Sciences, Free University of Berlin, 12249 Berlin, Germany
School of Earth and Environment, University of Leeds, Leeds LS2 9JT, UK

M. Kellermeier (✉)
Material Physics, BASF SE, Carl-Bosch-Str. 38, D-67056 Ludwigshafen, Germany
e-mail: matthias.kellermeier@basf.com

of the key observations supporting these alternative crystallization mechanisms were derived for (bio)minerals such as calcium carbonate or calcium phosphate, due to their great relevance for global carbon cycling and ocean chemistry as well as biomimetic materials chemistry, as was documented in many of the previous chapters in this book. In the quest to better understand such alternative pathways, other likewise important minerals have been neglected and only slowly these move into the focus of more detailed investigation. One such example is calcium sulfate, a compound of considerable interest for both industrial applications and geological environments. Recent studies have indicated that the formation of this mineral can also occur via a multistage pathway, again confirming that the crystallization of sparsely soluble salts is far more complex than pictured by standard models found in general mineralogy textbooks.

The foremost aim of this chapter is to review the current state of knowledge on the process of calcium sulfate precipitation from solution. Following a brief introduction to the mineralogy and relevance of calcium sulfates, we will focus on two main aspects: (1) the phase diagram of the $\text{CaSO}_4\text{-H}_2\text{O}$ system (including solubilities and relative stabilities of the different mineral phases as a function of temperature, pressure, and salinity) and (2) the mechanisms of CaSO_4 nucleation and growth, both from a classical perspective and in view of recently gained insights, again considering the influence of different solution conditions. Eventually, an attempt will be made to unify the various reported observations toward an integrated model for the formation of calcium sulfates, not forgetting however to also highlight some central questions still open for further research.

12.1.1 CaSO_4 Mineralogy and Structure

Calcium sulfate can exist in various structural forms. In the presence of water, three distinct crystalline phases occur, differing in their degree of hydration: gypsum, the dihydrate ($\text{CaSO}_4 \cdot 2\text{H}_2\text{O}$), bassanite, the hemihydrate ($\text{CaSO}_4 \cdot 0.5\text{H}_2\text{O}$), and anhydrite, the anhydrous form (CaSO_4). The crystal structures of these three main phases are shown in Fig. 12.1. In addition to the water content, there are further structural and/or morphological differences between crystals belonging to the respective hydrate family (Table 12.1). Anhydrite, for example, comprises three different polymorphs: (1) the AIII phase, or γ -anhydrite, with hexagonal symmetry (obtained when water is quantitatively removed from bassanite by drying, but generally metastable); (2) the AII phase, or β -anhydrite, with orthorhombic symmetry (the thermodynamically stable phase at temperatures <1200 °C); and (3) the AI phase, or α -anhydrite, with trigonal symmetry (formed when β -anhydrite is heated above 1200 °C and replacing β -anhydrite as stable phase at higher temperatures) (Chang et al. 1996).

Since orthorhombic anhydrite is the only phase that precipitates spontaneously from aqueous solutions, the other polymorphs will not be considered further in this chapter.

In the case of bassanite, there is a distinction into α - and β -hemihydrate based on the way of production (Lewry and Williamson 1994; Singh and Middendorf 2008).

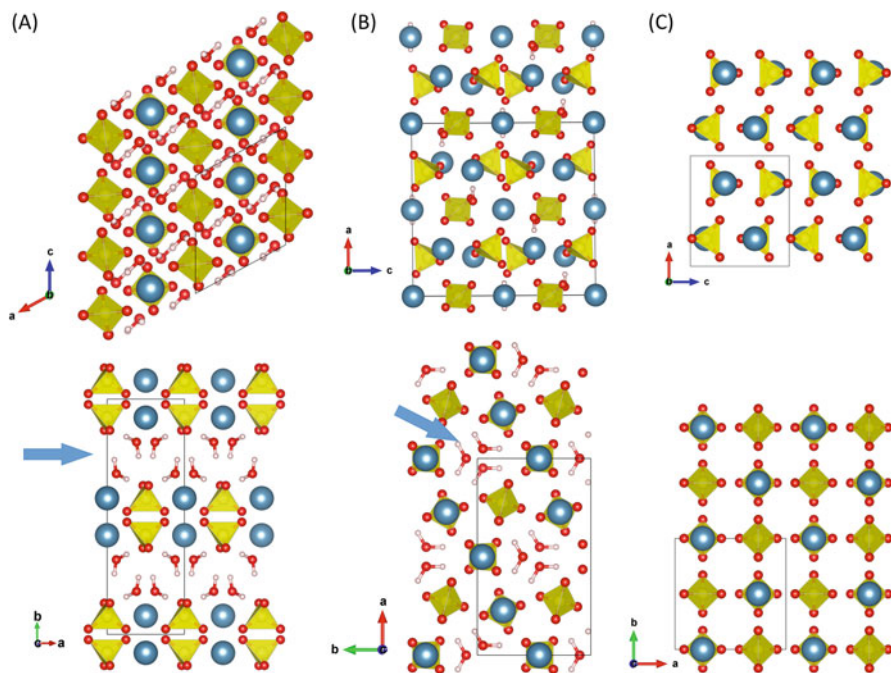


Fig. 12.1 Structural motifs of the three main calcium sulfate phases, gypsum, bassanite, and anhydrite (All form). Tetrahedra are sulfate ions, large spheres are Ca ions, and arrows indicate water sheets and channels in the gypsum and bassanite structures, respectively (Images were drawn with VESTA (Momma and Izumi 2011))

The two types of bassanite differ primarily with respect to the shape of the crystals (α being more prismatic than β), their reactivity in contact with water (Lewry and Williamson 1994), and the mechanical properties of the final product (Satava 1970). Whether or not there are true structural differences between the two forms is still under debate (Singh and Middendorf 2008, and references therein). In addition, it has been reported that the actual water content in the bassanite structure can vary over a quite broad range ($\text{CaSO}_4 \cdot x\text{H}_2\text{O}$, where $0 \leq x \leq 0.8$, in particular 0.5–0.8), likely due to the fact that variable amounts of water can be accommodated in the channels of the lattice (which at low values of x resembles that of γ -anhydrite) (Abriel 1983; Lager et al. 1984). However, based on single-crystal refinement and structure optimization by DFT calculations, a recent study concluded that hemihydrate should contain exactly 0.5 water molecules per formula unit and that subhydrates with a crystal water content of more than 0.5 per CaSO_4 are unlikely (Weiss and Bräu 2009).

12.1.2 Calcium Sulfate in Natural Environments

Gypsum and anhydrite are the most abundant sulfate minerals in the Earth's crust and frequently occur in evaporitic environments (e.g., Warren 2006), such as the

Table 12.1 Overview of the different calcium sulfate phases

Phase	Common name(s)	Formula	Stability range	Remarks
Gypsum	Selenite, alabaster	$\text{CaSO}_4 \cdot 2\text{H}_2\text{O}$	<60–90 °C in air <40–60 °C in H ₂ O	Formed spontaneously upon precipitation from solution under ambient conditions
Bassanite	Hemihydrate	$\alpha\text{-CaSO}_4 \cdot 0.5\text{H}_2\text{O}$	Metastable in H ₂ O	Formed by heating gypsum in air at >60–90 °C; readily rehydrates to gypsum
	Plaster of Paris	$\beta\text{-CaSO}_4 \cdot 0.5\text{H}_2\text{O}$	Metastable in H ₂ O	Formed by heating gypsum in water at >90 °C; readily rehydrates to gypsum
Anhydrite	AIII, Soluble anhydrite	$\gamma\text{-CaSO}_4$	Metastable in H ₂ O and air	Formed by heating gypsum in air at >100–130 °C; readily rehydrates to hemihydrate or gypsum
	AII, Insoluble anhydrite	$\beta\text{-CaSO}_4$	Stable <~1200 °C	Natural anhydrite formed at the Earth's surface
	AI	$\alpha\text{-CaSO}_4$	Stable >~1200 °C	Converts immediately into $\beta\text{-CaSO}_4$ on cooling below ~1200 °C

Modified after Osinski and Spray, 2003

large deposits formed during the Messinian salinity crisis event (~5.3 million years ago), during which the majority of the Mediterranean evaporated and produced huge amounts of gypsum (Ryan 2009). Both gypsum and anhydrite are also present in low-temperature hydrothermal zones (Blount and Dickson 1969), with one spectacular example being the giant gypsum crystals found along with considerable amounts of anhydrite inside the Naica Mine in Chihuahua, Mexico (Garcia-Ruiz et al. 2007; Van Driessche et al. 2011). Recently, considerable quantities of gypsum have also been discovered on Mars (Langevin et al. 2005). As opposed to gypsum and anhydrite, bassanite is a very rare mineral on Earth (Allen and Kramer 1953; Apokodje 1984; Peckmann et al. 2003), but significant amounts have been detected on Mars (Wray et al. 2010) as well as in Martian meteorites (Ling and Wang 2015).

In addition to the geological occurrences mentioned above, calcium sulfates can also be found as structural components associated with living organisms. For example, two classes of medusae (Scyphozoa and Cubozoa) use bassanite

for gravitational sensing (Tienmann et al. 2002; Becker et al. 2005; Boßelmann et al. 2007), and there is evidence for the presence of bassanite in the so-called “toothbrush” tree in Africa (Dongan et al. 2005). Also noteworthy is the frequent occurrence of gypsum-rich microbialites (e.g., stromatolites), both in past- and present-day evaporitic environments (Rouchy and Monty 2000). However, the role that microorganisms played in the formation of these structures is still under debate. In any case, compared to carbonates (see Falini and Fermani 2017, Chap. 9), phosphates (see Birkedal 2017, Chap. 10; Delgado-Lopez and Guagliardi 2017, Chap. 11), silicates (see Tobler et al. 2017, Chap. 15), or iron oxides (see Reichel and Faivre 2017, Chap. 14; Penn et al. 2017, Chap. 13), the number of living organisms that decided on sulfates as their biomineral of choice is minimal.

12.1.3 Relevance of Calcium Sulfate for Industrial Applications

Calcium sulfate is an important industrial material, with more than 100 million tons annually consumed worldwide (Sharpe and Cork 2006). While gypsum and anhydrite are mainly extracted from their abundant natural resources (or gained as by-products of other processes, e.g., in the industrial synthesis of several acids or during flue-gas desulfurization in coal-fired power plants), bassanite is usually obtained by partial dehydration of gypsum through heating at temperatures between 80 and 180 °C. Despite this cost- and energy-intensive process, hemihydrate remains one of the most extensively produced inorganic materials due to its relevance for the construction industry, where it is used on large scales as a binder in cements, mortars, or stucco (bassanite is often referred to as *plaster of Paris*). Anhydrite is likewise a common component of cementitious products like binders or adhesives. Finally, gypsum finds broad application in the agricultural (e.g., as soil conditioner), food (e.g., as flocculant), and pharmaceutical (e.g., as inert filler material) sectors (Sharpe and Cork 2006). Given this wide scope of possible uses, it is evident that there is an industrial demand for the design of simple and efficient protocols providing control over the phase composition, size, and morphology of CaSO_4 crystals, which may be achieved via solution precipitation if the underlying mechanisms are properly understood.

On the other hand, solid calcium sulfates also pose a severe problem to the industrial sector, as they represent recurrent scalants in several important processes, such as water purification in desalination plants, oil recovery, and mining activities (Ahmed et al. 2004; Mi and Elimelech 2010, Lu et al. 2012). Here, unwanted precipitation in pipes and on heat exchanger surfaces leads to incrustation, which causes a loss of efficiency or even costly downtimes for cleaning (with anhydrite being the major scale-forming phase at temperatures >100 °C and gypsum prevailing at lower temperatures). Therefore, considerable efforts are made to develop advanced strategies to prevent or retard crystallization under process conditions, which again

demands (or at least would benefit from) detailed insights into the mechanisms at work. Another challenge related to calcium sulfates is the role that gypsum crystallization plays in the deterioration of building materials (e.g., concrete, mortar, marble, etc.) during sulfate (Neville 2004) or acid (Charola et al. 2007) attack. The latter is of increasing importance due to the continuing acidification of rainwater.

12.2 The $\text{CaSO}_4\text{-H}_2\text{O}$ Phase Diagram

12.2.1 Solubility

In order to understand, and eventually control, the precipitation of calcium sulfates from solution, it is essential to know the phase diagram of the system, as this provides thermodynamic information on relative phase stabilities. Together with kinetic factors, these will determine the outcome of any crystallization process. The intersections of the solubility curves of different possible phases indicate the transition temperatures and thus define their corresponding thermodynamic stability field during precipitation from aqueous solution. Precise knowledge of these transition temperatures is of great relevance for understanding under which conditions evaporites (gypsum/anhydrite) have formed in the geological record, but equally also for optimizing the production/application of calcium sulfate-based materials (gypsum/bassanite and anhydrite/bassanite) in industrial processes. Not surprisingly, the solubility of solid CaSO_4 phases has been investigated extensively, with the first systematic works on the $\text{CaSO}_4\text{-H}_2\text{O}$ system dating back to the late nineteenth century (e.g., Marignac 1874; Raupenstrauch 1885), followed by a plethora of studies in the twentieth century. Considerable effort was also devoted to the solubility in multicomponent systems, i.e., in the presence of other salts (e.g., Posnjak 1938; Bock 1961), and the effect of pressure (e.g., Dickson et al. 1963; Monnin 1990). Figure 12.2 shows a comprehensive overview of the solubility of the three relevant phases as a function of temperature and salinity, including both experimental and calculated data (using the PHREEQC speciation software (Parkhurst and Appelo 1999)).

Although most experimental measurements are in relatively good agreement with each other, still a considerably broad range of solubility data exists for all three phases (shaded areas in Fig. 12.2a). Quite remarkably, the same conclusion has already been drawn as early as 1902 by Hulett and Allen, who stated: “Although the solubility of the substance CaSO_4 has been the subject of investigation by many careful workers, the results vary widely, while the experimental errors are comparatively small.” The marked spread among the reported experimental solubility values, as well as those derived from thermodynamic predictions, leads to a distinct uncertainty in the transition temperatures of gypsum to anhydrite and hemihydrate to anhydrite. Consequently, the stability regions of the different phases in the $\text{CaSO}_4\text{-H}_2\text{O}$ system are still rather ill-defined.

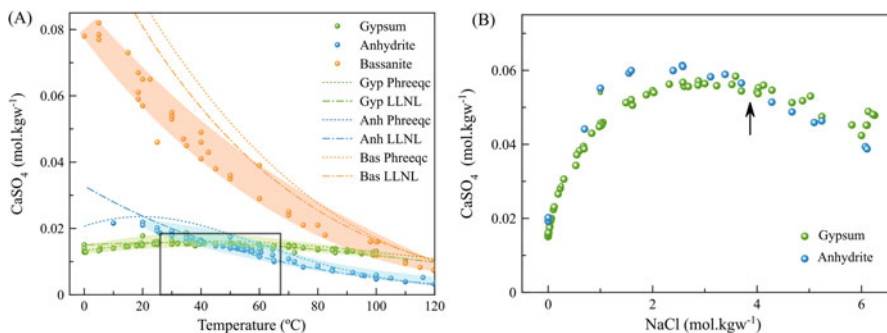


Fig. 12.2 Solubility curves for (a) gypsum, bassanite, and anhydrite (AII form) in pure water at different temperatures and (b) gypsum and anhydrite (AII form) as a function of salinity at ambient temperature. Both plots contain experimental data extracted from the literature (dots). The lines in (a) represent solubility curves calculated using the PHREEQC (dotted lines) and LLNL (dot-stripe lines) databases. The shaded areas in (a) are a visual aid highlighting the range of the reported experimental solubility data. The black box in (a) highlights the uncertainty range of the gypsum/anhydrite transition temperature. The black arrow in (b) marks the expected transition temperature at 25 °C and ~4 M NaCl. Experimental data were taken from: Poggiale (1843), Marignac (1874), Droeze (1877), Tilden and Shenstone (1984), Raupenstrauch (1885), Boyer-Guillon (1900), Cameron (1901), Hulet and Allen (1902), Melcher (1910), Hall et al. (1926), Hill (1937), Hill and Wills (1938), Partridge and White (1929), Roller (1931), D’Ans (1933, 1968), Booth and Bidwell (1950), Madgin and Swayles (1956), Bock (1961), Dickson et al. (1963), Marshall et al. (1964), Zen (1965), Marshall and Slusher (1966), Power et al. (1964, 1966), Block and Waters (1968), Blount and Dickson (1969, 1973), Culberson et al. (1978), Innorta et al. (1980), Kontrec et al. (2002), and Azimi and Papangelakis (2010)

12.2.2 Phase Transition Temperatures

Gypsum/Anhydrite The temperatures for the gypsum/anhydrite transition have been extensively studied due to its relevance for understanding the evolution of evaporitic deposits. Van’t Hoff and coworkers were the first to address this issue in detail using experimental measurements and thermodynamic calculations and proposed a range of 60–66 °C for the transition temperature (van’t Hoff et al. 1903; see also black box in Fig. 12.2a). Since then, a large number of related experimental and theoretical studies have been performed. The resulting transition temperatures are summarized in Table 12.2. They can be roughly divided into two groups, centered around 42 and 58 °C, respectively. The main challenge, standing in the way of a more precise determination of the transition temperature, is the very slow dissolution/growth kinetics of anhydrite at temperatures lower than ~80 °C, i.e., anhydrite remains metastable in either under- or supersaturated solution and true thermodynamic equilibrium is difficult (or even impossible) to reach in a reasonable period of time. One way to circumvent this problem is to precisely measure anhydrite solubility at higher temperatures (faster kinetics) and then extrapolate to lower temperatures. However, this method also suffers from obvious drawbacks (such as the extrapolation of data) and depends on precise knowledge

Table 12.2 Reported values for the gypsum/anhydrite transition temperature in water

Authors	Transition temperature/°C	Method
Van't Hoff et al. (1903)	60–66	Experiments and thermodynamic calculations
Partridge and White's (1929)	38–39	Solubility measurements of anhydrite at high temperature and extrapolation
Hill (1937)	42 ± 1	Solubility measurements of anhydrite at lower temperatures (65, 45, and 35 °C) and interpolation
Posnjak (1938)	42 ± 2	Solubility measurements
Kelly et al. (1941)	40	Measurements of thermochemical properties of solid gypsum and anhydrite and calculation of the transition temperature
Bock (1961)	42	Solubility measurements of anhydrite and gypsum
Marshall et al. (1964)	42	Solubility measurements
Zen (1965)	46 ± 25	Calculations based on revised thermodynamic data of Kelly et al.
Power et al. (1966)	41 ± 1	Solubility measurements of gypsum and anhydrite
Hardie (1967)	58 ± 2	Water activity measurements
Blount and Dickson (1973)	56 ± 3	Solubility measurements of anhydrite at high temperature (>70 °C) and extrapolation
Knacke and Gans (1977)	55.5 ± 1.5	Equilibration experiments in solutions containing both gypsum and anhydrite
Innorta et al. (1980)	49.5 ± 2.5	Solubility measurements
Corti and Fernandez-Prini (1983)	42.6 ± 0.4	Thermodynamic calculations
Hamad (1985)	46	Solubility measurements at high pressure and extrapolations to 1 atm
Raju and Atkinson (1990)	59.9	Thermodynamic calculations
Kontrec et al. (2002)	40	Solubility measurements and phase transition experiments
Azimi et al. (2007)	40 ± 2	Modeling of CaSO ₄ solubility

of the solubility of gypsum, which itself is subject to uncertainties (cf. Fig. 12.2a). Using thermodynamic parameters to calculate the transition temperature is also not a more reliable approach, because these parameters themselves rely on solubility data. In summary, there is still considerable ambiguity with respect to the correct temperature for the gypsum-to-anhydrite transition, and as discussed by Freyer and Voigt (2003), there are no obvious reasons to prefer one group of values over the other.

Gypsum/Bassanite Considerably less attention has been paid to the gypsum/bassanite transition temperature due to the fact that at Earth's surface conditions, bassanite is metastable, i.e., at the conditions where gypsum transforms

to bassanite, anhydrite is actually the stable phase (cf. Fig. 12.2a). However, anhydrite does not readily form due to much slower nucleation and growth kinetics (Ossorio et al. 2014). Moreover, the exact value of the gypsum/bassanite transition temperature seems to be of little relevance to natural phenomena. However, it is very well important for the production process of plaster of Paris and other industrial hemihydrate materials. Within the range of reported solubility data, the possible gypsum/bassanite transition temperature may vary from less than 80 to nearly 110 °C (cf. Fig. 12.2a). From dilatometric and tensiometric measurements, van't Hoff and coworkers (1903) derived a transition temperature of 106 °C, while Posnjak (1938) obtained 97 ± 1 °C using solubility data of bassanite and gypsum, which is close to the 98–100 °C reported by Partridge and White (1929). By modeling the solubility of CaSO_4 phases, Azimi et al. (2007) determined the transition temperature to be 99 ± 2 °C. These studies suggest that there is generally much better agreement about the transition temperature of gypsum to bassanite compared to that of gypsum to anhydrite.

Anhydrite/Bassanite In the case of the transition between bassanite and anhydrite, it is assumed that bassanite remains metastable (i.e., more soluble than anhydrite) over the entire relevant temperature range (~ 50 – 1200 °C). Thus, no distinct crossover temperature has been reported so far (Kontrec et al. 2002). Although solubility data of hemihydrate at higher temperatures (>100 °C) are very close to those of anhydrite, stability experiments show that bassanite transforms into anhydrite in contact with aqueous solution when given enough time (e.g., 1 week at 99 °C and 0.8 M NaCl) (Ossorio et al. 2014).

12.2.3 *Influence of Salt and Pressure on Calcium Sulfate Solubility*

So far, we have only considered the CaSO_4 – H_2O system at atmospheric pressure (except for the solubility data of bassanite and anhydrite above 100 °C) and in relatively pure systems without any additional salts or other solutes. Indeed, there is a vast array of studies that assessed the solubility of gypsum in ternary and quaternary systems (Azimi et al. 2007, Azimi and Papangelakis 2010, and references therein). The best-documented case is the solubility of CaSO_4 in the presence of sodium chloride (Fig. 12.2b). As NaCl is added to solutions of gypsum, a sharp increase in solubility is observed from 0 to 1 M; this can be ascribed to the concurrent decrease in the activity coefficients of Ca^{2+} and SO_4^{2-} , which increases the dissolved concentration at a given constant solubility product (as indicated by calculations with PHREEQC). At higher NaCl concentrations, first a maximum is reached between 2 and 3 M, before a slight decrease occurs at still higher salt contents. The solubility of gypsum in the presence of a large variety of other salts has also been measured and modeled, but a detailed discussion of these effects is beyond the scope of this chapter.

The dependency of solubility on ionic strength is slightly different for anhydrite, especially at low temperatures, leading to a crossover at high salt concentrations (cf. Fig. 12.2b) and suggesting that anhydrite should be the stable phase at room temperature and high salinity. Hence, with increasing NaCl concentration the gypsum/anhydrite transition temperature is shifted progressively to lower temperatures (Bock 1961). Interestingly, so far no experiments have been reported to confirm the spontaneous formation of anhydrite under these conditions; quite the contrary, Cruft and Chao (1970) and Ossorio et al. (2014) found that up to ~ 70 °C gypsum or bassanite are always the primary phases obtained due to kinetic inhibition of anhydrite formation.

Finally, it is well established that the solubilities of both gypsum and anhydrite increase with pressure. For example, at 50 °C the solubility of gypsum is about 15 mM at 1 bar and ca. 35 mM at 1000 bar, while at 80 °C anhydrite has a solubility of ca. 9 and 25 mM at 1 and 1000 bar, respectively (Blount and Dickson 1973). In the case of anhydrite, the presence of other salts strongly influences this dependency, making the pressure-solubility relation more complex (Blount and Dickson 1969).

12.3 CaSO₄ Formation from Solution

Similar to the solubility of calcium sulfate, its precipitation from solution has been the subject of extensive studies, again due to the importance of corresponding processes in both natural and industrial settings. In this section, we will discuss the state of the art of CaSO₄ mineralization from different perspectives. The first, and most comprehensive part, deals with precipitation from aqueous environments at low temperatures (<60 °C), where gypsum is the thermodynamically stable phase. The second part will focus on precipitation at higher temperatures, where bassanite and anhydrite are the dominant phases. In the third part, we discuss the influence of additives on CaSO₄ mineralization, before finally we attempt to reconcile the various observations and integrate them into a general model for the crystallization of calcium sulfate.

12.3.1 Nucleation and Growth of Gypsum

12.3.1.1 The “Classical” Picture

The first systematic studies on the precipitation of CaSO₄ from aqueous solutions were performed during the late nineteenth and early twentieth century, mostly focusing on solubility measurements (as described above). Later on, driven by the industrial and geological interests, a large number of papers were published on the nucleation and growth of gypsum, the kinetics of the transformation of bassanite

to gypsum (i.e., the hydration process of corresponding binders in construction materials), and the relative phase stabilities in the $\text{CaSO}_4\text{-H}_2\text{O}$ system. These early studies broadly agreed that gypsum precipitation from a supersaturated solution proceeded via a two-stage process (Conley and Boundy 1958; Schierholtz 1958; Smith and Sweett 1971): (I) formation of incipient (more or less) crystalline nuclei and (II) growth of these nuclei into gypsum crystals – i.e., the classical view of crystallization (Kashchiev 2000).

Induction time measurements performed by Liu and Nancollas (1973) suggested that the nucleation of gypsum is associated with an appreciable activation barrier, involving a critical nucleus composed of approximately six ions, as predicted based on a “nonclassical nucleation model” introduced by Christiansen and Nielsen (1952). On the other hand, Packter (1971) measured induction times as well as numbers and final sizes of crystals to conclude that gypsum formed through a heterogeneous process, in which nuclei are generated rapidly (almost immediately after mixing the reagents) on dust particles suspended in the supersaturated solution. Growth was then suggested to occur initially through a slow “mononuclear” process, yielding small crystallites that persisted over prolonged induction periods (which is equivalent to the large activation barrier mentioned above). These primary particles were finally thought to grow into large gypsum crystals by a more rapid “polynuclear” mechanism. Overall, this proposed scheme appears to be inspired by the precipitation model for sparingly soluble metal salts in solutions of low supersaturation presented by Nielsen (1964).

More recently, a large number of studies were performed with the aim to precisely measure induction times of gypsum precipitation as a function of parameters like supersaturation or temperature and/or in the presence of additives at different concentrations (e.g., Klepetsanis and Koutsoukos 1989; Hamdona et al. 1993; He et al. 1994; Klepetsanis et al. 1999; Lancia et al. 1999; Prisciandaro et al. 2001a, b; Alimi et al. 2003; Prisciandaro et al. 2003; Rashad et al. 2004; Fan et al. 2010). In essence, these studies concluded that the formation of gypsum appears to be reasonably well described by the classical nucleation theory (CNT), with nucleation kinetics being strongly dependent on temperature and solution speciation (like for many other insoluble salts). In most cases, the experimental data were fitted by the CNT equation and separated the into two regimes, i.e., homogeneous nucleation at high levels of supersaturation and heterogeneous nucleation at lower supersaturation. From these fits, the effective surface free energies of the forming nuclei was obtained, yielding rather realistic values of ~ 40 mJ/m^2 and ~ 14 mJ/m^2 for homogeneous (He et al. 1994; Lancia et al. 1999; Alimi et al. 2003; Fan et al. 2010) and heterogeneous (Alimi et al. 2003) nucleation, respectively.

This highlights that even though the particular mechanisms underlying nucleation may involve species that are fundamentally distinct from those envisaged in the classical picture of crystallization (see below), CNT can still provide a good description of the kinetics of the process – i.e., “nonclassical” nucleation does not necessarily mean that CNT is not valid (note that CNT was actually developed for the case of liquid condensation from vapors (e.g., Becker and Döring 1935) and hence it should be equally well, or even more, applicable to liquid/amorphous nuclei

than to crystalline nuclei). This notion is of course not unique to calcium sulfate, but may generally be considered for a large variety of mineral systems (see e.g. De Yoreo et al. 2017, Chap. 1).

Indeed, none of the aforementioned investigations provided direct insight into the actual pathway(s)/mechanism(s) of the nucleation process. Thus, despite the large amount of data on gypsum precipitation collected over the years, the nature of the relevant species and their spatiotemporal evolution were still largely unknown at the beginning of this century. Instead, it was inherently assumed that CaSO_4 nucleation is a one-step process, which according to the classical paradigm directly produces nuclei that have the same characteristics (e.g., order, density, composition, etc.) as the fully grown (macroscopic) crystals (Kashchiev 2000).

12.3.1.2 Recent Observations: “Non-Classical” Processes

Sparked by the significant advances made for prominent mineral systems like calcium carbonate (De Yoreo et al. 2017, Chap. 1; Wolf and Gower 2017, Chap. 3; Fernandez-Martinez et al. 2017, Chap. 4; Rodriguez-Blanco et al. 2017, Chap. 5; Demichelis et al. 2017, Chap. 6; Andreassen and Lewis 2017, Chap. 7; Rao and Cölfen 2017, Chap. 8, and references therein) or calcium phosphate (Birkedal 2017, Chap. 10; Delgado-Lopez and Guagliardi 2017, Chap. 11, and references therein), various groups started to explore if a more complex crystallization pathway may underlie the precipitation of calcium sulfate. And indeed, the past few years have seen a growing body of evidence supporting the notion of multistage processes governing the formation of gypsum from aqueous solutions. In the following, we provide an overview of these new insights and discuss their implications for the emerging new picture of calcium sulfate mineralization at ambient conditions.

In 2012, Wang et al. (2012) reported on the existence of precursor phases during gypsum crystallization. They precipitated CaSO_4 at room temperature by mixing equimolar aqueous solutions of CaCl_2 and Na_2SO_4 , and the formed solid particles were isolated at regular time intervals from the reacting solutions and characterized in the dry state by TEM and a number of complementary methods. Under the conditions tested, evidence was found for a short-lived amorphous phase appearing almost immediately after mixing solutions containing 25 mM CaSO_4 . This conclusion was based on the fact that the isolated solids did not produce distinct crystalline spots when analyzed by selected-area electron diffraction (SAED) and that they readily transformed into gypsum upon prolonged exposure to the electron beam. Furthermore, samples isolated from a 50 mM solution (supersaturated with respect to gypsum but undersaturated with respect to bassanite) suggested that bassanite can form under conditions where it should not and remained stable for at least 1 h after mixing. Therefore, it was proposed that initially an amorphous calcium sulfate (ACS) phase formed that then converted into gypsum *via* bassanite as an intermediate crystalline stage. Moreover, the data suggested that both the amorphous precursor and the bassanite intermediate became progressively less stable (shorter

lifetimes) with increasing supersaturation, and thus it was hypothesized that at high supersaturation, gypsum may form directly from solution.

At the same time, Van Driessche et al. (2012) used time-resolved turbidity measurements combined with *ex situ* characterization by high-resolution TEM and nano-diffraction to probe the early stages of calcium sulfate precipitation from mixtures of Na_2SO_4 and CaCl_2 at different levels of supersaturation. Based on the turbidity results, the precipitation process was arrested at different times by quenching the reaction through flash-freezing of solution aliquots or by addition of ethanol to wet particles obtained by micro-filtration. From detailed HR-TEM analyses, it was inferred that gypsum was formed via a three-stage process: (1) homogeneous nucleation of ca. 5 nm primary nanocrystalline bassanite particles and growth of these particles to about 100 nm; (2) self-assembly of the as-formed bassanite nanoparticles into elongated aggregates, co-oriented along their *c*-axis (i.e., oriented attachment); and (3) collective transformation of these aggregates into gypsum by merging of the bassanite units into a common crystallographic register along high-energy faces (Zhang and Banfield 2012). In the study of Van Driessche et al. (2012), no evidence of an amorphous CaSO_4 precursor phase was found. Moreover, the exact mechanism by which the oriented aggregates transformed into gypsum remained unresolved. However, it was suggested that there might be a crossover in the thermodynamic stability of calcium sulfate phases at small particle sizes, with bassanite becoming more stable than gypsum at the nanoscale under ambient conditions. This notion is similar to what has been proposed for the CaCO_3 system in the pioneering work of Navrotsky (2004).

Further observations supporting the idea of a multistage precipitation pathway for gypsum were reported by Saha et al. (2012). They used time-resolved cryogenic transmission electron microscopy (cryo-TEM) to probe the early stages of particle formation in a solution supersaturated with respect to gypsum, obtained by dissolution of bassanite. They observed small nanoclusters (2–4 nm in size) that evolved to seemingly amorphous particles (ca. 100 nm in diameter), which later reorganized to yield crystalline gypsum. On the whole, this multistep process took place on timescales on the order of tens of seconds.

Finally, at the end of 2012, Jones reported about an interesting study where attenuated total reflection (ATR) Fourier transform infrared (IR) spectroscopy was used to follow *in situ* the crystallization behavior of CaSO_4 in solution upon evaporation (Jones 2012). It was found that the intensity of IR bands corresponding to structural water increased over time, indicating that water molecules initially occupied disordered positions (in an assumed amorphous CaSO_4 phase). In later stages, the water molecules adopted more defined configurations characteristic of the forming of crystalline solids (inferred to be bassanite and/or gypsum). It was also noted that the presence of water might influence the stability of the initial disordered phase. Thus, Jones (2012) concluded that the crystallization process started with a disordered (“amorphous”) phase that slowly transformed into crystalline gypsum, possibly via a bassanite intermediate. During this transformation, water seems to play a key role, shifting from disordered to ordered positions and thus inducing the emergence of a defined crystal lattice.

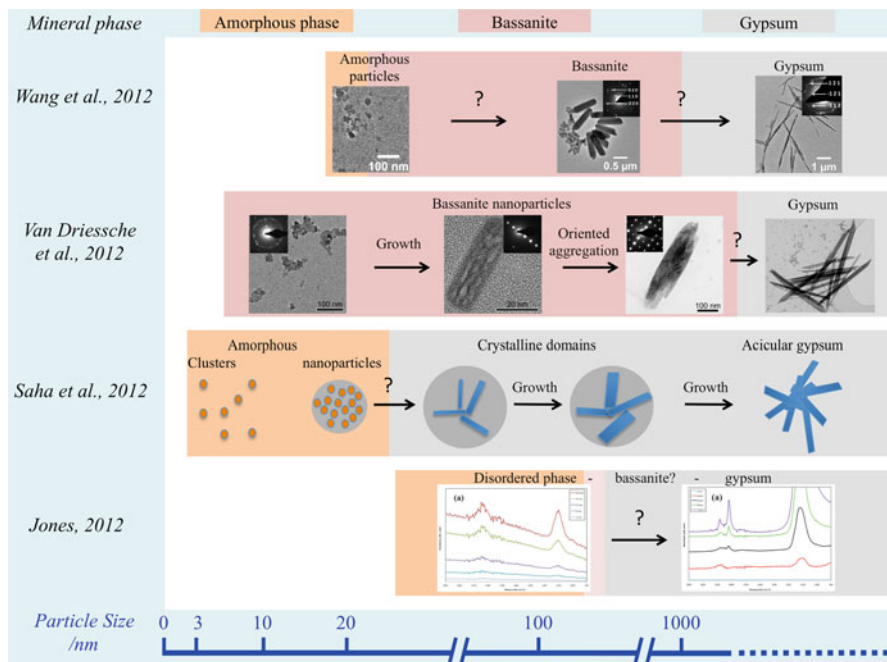


Fig. 12.3 Schematic overview of the various precursor phases and pathways leading to gypsum formation from aqueous solutions at room temperature, as recently proposed by Wang et al. (2012), Van Driessche et al. (2012), Saha et al. (2012) and Jones (2012). Note that the in the online version different phases are color-coded and that the respective phase sequences are arranged according to changes in size (bottom axis), not time

Although all these studies addressed the same problem, the results still show discrepancies, likely because of inherent differences in the used experimental and analytical approaches. Nevertheless, it seems clear that there are alternative pathways to crystalline gypsum from supersaturated aqueous solutions other than direct nucleation and growth as envisaged in the classical picture. The general conclusion is that the phase(s) formed initially upon precipitation from solution can be quite distinct from the final crystalline state (gypsum), or in other words that gypsum formation indeed involves one or more precursor/intermediate phases. Figure 12.3 provides an overview of the reaction sequences proposed in the recent studies discussed above.

It is important to note that the reported data are ambiguous with respect to the question whether amorphous precursors or bassanite nanoparticles, or both, play a key role in the formation of gypsum. The main reason for these ambiguities lies in the fact that it is extremely difficult to capture the elusive early stages of precipitation with sufficient temporal and spatial resolution, while at the same time not affecting the state of the reacting solids and solutions. Although some

of the described studies used in situ methods (i.e., IR spectroscopy or turbidity measurements), these lack specific resolution and provide limited information about size, shape, or crystallinity of the formed solids. In turn, the applied ex situ techniques provide sufficient resolution (e.g., (cryo)-TEM) but suffer from the obvious drawback of possible sample preparation artifacts, along with other problems like beam damage. These difficulties may lead to a situation where the detected particles are actually not present in solution but rather formed/transformed during isolation and/or analysis. Indeed, the strategies used for sample preparation in the abovementioned studies (including micro-filtration, cryo-quenching, or direct analysis of cryo-vitrified samples) are designed to minimize undesirable effects, but still they do not offer true in situ and time-resolved characterization of the occurring processes, as would be needed to fully address these rapidly evolving reactions in the CaSO_4 system at the proper length scale.

This limitation was just recently circumvented by Stawski et al. (2016), who combined synchrotron-based small- and wide-angle X-ray scattering (SAXS/WAXS) to investigate gypsum formation from supersaturated solutions. These in situ experiments were carried out over a temperature range of 12–40 °C, by direct mixing of equimolar Na_2SO_4 and CaCl_2 solutions and circulating the resulting samples through a capillary centered in the X-ray beam. In-depth evaluation of the obtained data led to the conclusion that crystalline gypsum forms via a multistep process, involving four well-defined stages (see Fig. 12.4):

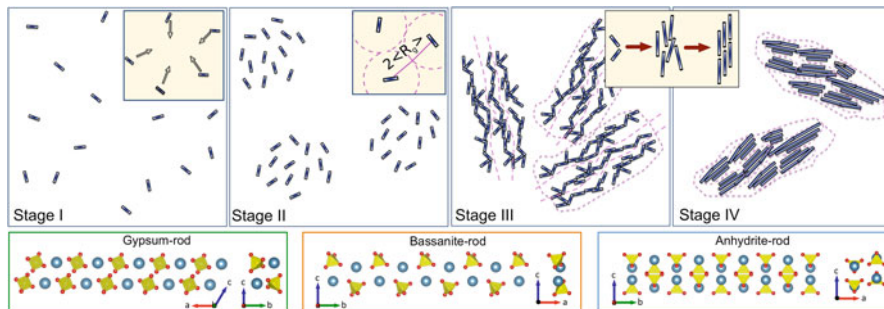


Fig. 12.4 Schematic representation of the four stages of CaSO_4 precipitation from solution as proposed by Stawski et al. (2016) based on the results of in situ SAXS/WAXS experiments: Stage I, formation of sub-3 nm primary species. Stage II, assembly of the primary species into loose domains; the inset shows that individual scatterers are separated by a distance larger than two times the radius of gyration. Stage III, further aggregation into large surface-fractal morphologies. Stage IV, growth and coalescence of the primary species within the aggregates and transformation to gypsum. The inset between stages III and IV shows the successive evolution at the nano- and mesoscale, where the primary units first grow/coalesce in length and subsequently in all dimensions, yielding structural domains of increasing size and crystallinity. The three panels on the bottom show tentative molecular structures for the anhydrous rodlike primary species based on the gypsum, bassanite, and anhydrite lattice

- (Stage I) Formation of elongated primary species, <3 nm in length and ~ 0.5 nm in diameter and composed of “anhydrous” Ca-SO_4 cores (as indicated by considerations of SAXS volume fractions and electron densities)
- (Stage II) Assembly of these primary species via density fluctuations into loose domains, where the interparticle distance remains still fairly large, i.e., >2 times the radius of gyration of the individual primary particles
- (Stage III) Further condensation of these domains into larger and denser aggregates, still consisting of the same primary units
- (Stage IV) Growth of the primary units within the aggregates, mutual alignment, and eventual collective reorganization/transformation into gypsum, as confirmed through the simultaneously collected WAXS data

These results suggest that CaSO_4 precipitation from solution relies on the formation and aggregation of nanosized primary units with a rather well-defined size and composition – which may or may not be analogous to the so-called “pre-nucleation clusters” reported for the calcium carbonate and phosphate systems (Gebauer et al. 2008; Dey et al. 2010; Kellermeier et al. 2014). So far no data are available on how stable or metastable these primary CaSO_4 species are. In any case, the structure of the primary units cannot be uniquely assigned to any of the crystalline CaSO_4 phases (cf. bottom panels in Fig. 12.4). In other words, the primary species are equally similar to all three possible phases, and hence they may be considered as a universal precursor phase to any possible subsequent crystallization process. Under the conditions investigated by Stawski et al. (2016), the aggregation of the primary units into disordered domains and aggregates (Stages II and III) may correspond to either the “amorphous” phase reported in other studies (Wang et al. 2012; Saha et al. 2012; Jones 2012) or to the nanoparticulate bassanite observed in the works of Wang et al. (2012) and Van Driessche et al. (2012). We note that Stawski et al. (2016) could not unambiguously identify bassanite as a separate nanocrystalline intermediate in the solutions analyzed, possibly because the scattering units (or respectively their crystalline domains) present during Stages II and III were too small and/or not dense enough (large distance between individual units) to be detected by WAXS – or simply because bassanite is not an intermediate on the way to gypsum under the tested conditions.

A possible clue to the answer to this question has recently been reported by Tritschler et al. (2015a, b), who investigated the influence of organic (co)solvents on the precipitation behavior of calcium sulfate. By mixing supersaturated (but optically clear, i.e., metastable) aqueous CaSO_4 solutions with ethanol, nanoparticles of phase-pure bassanite were obtained (Fig. 12.5a) (Tritschler et al. 2015a). Similar observations were already made in an earlier study by Yang et al. (2011). These findings challenge the results of experiments where ethanol was used to supposedly quench the precipitation process in aqueous media (Wang et al. 2012; Van Driessche et al. 2012), as addition of the organic solvent may in fact induce the formation of bassanite rather than preserving structures that were thought to be present in solution before. Systematic variations of the water/ethanol ratio further showed that there is a critical water content (between 40 and 50 wt%), below which bassanite becomes

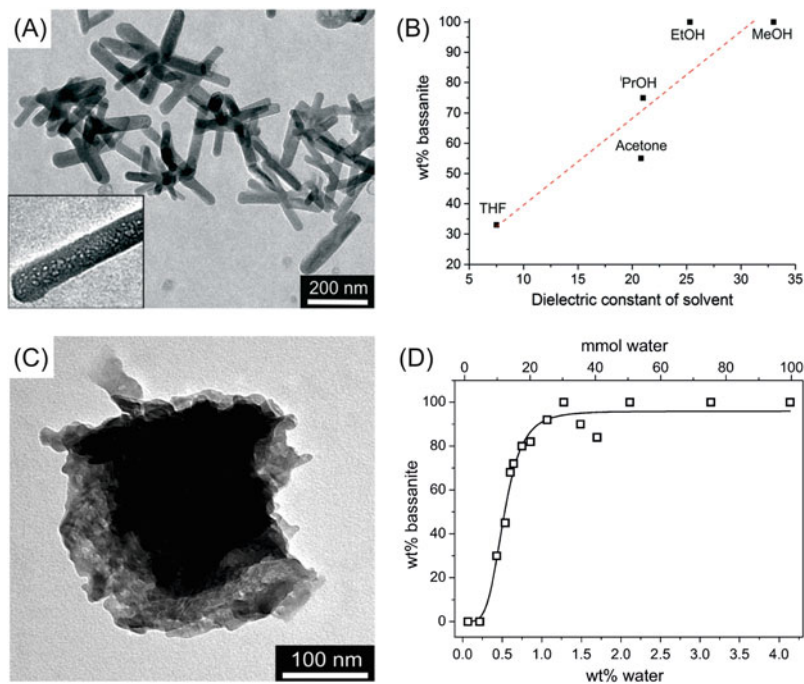


Fig. 12.5 Precipitation of calcium sulfate from mixtures of water and organic solvents. (a) Bassanite nanorods obtained by quenching 25 mM CaSO_4 solutions in an excess of ethanol. Note the morphological and structural similarity of the particles to those shown in Fig. 12.3. (b) Fraction of bassanite in mixtures with gypsum, as obtained by mixing aqueous CaSO_4 solutions with solvents of different polarity. (c) Phase-pure anhydrite produced by addition of concentrated sulfuric acid to solutions of CaCl_2 in methanol at an effective water content of 0.07 wt%. (d) Plot of the fraction of bassanite in mixtures with anhydrite as a function of the amount of water in the reaction medium (Figures are reproduced from (Tritschler et al. 2015a, b) with permission by the Royal Society of Chemistry and Wiley, respectively)

progressively favored over gypsum (Tritschler et al. 2015a). Another major factor for phase selection was found to be the type of organic solvent used for quenching, with more polar solvents yielding higher fractions of bassanite (Fig. 12.5b). This strongly suggests that the availability of water and the degree of hydration of any precursors (which is likely to depend on the polarity of the medium) are key factors for the outcome of the CaSO_4 precipitation process (as discussed in more detail below).

In a subsequent study, Tritschler et al. (2015b) extended this concept to significantly lower water contents and demonstrated that pure anhydrite (Fig. 12.5c) forms spontaneously at room temperature if less than 0.2 wt% water is present in mixtures with alcohol (Fig. 12.5d). Thus, it is possible to fine-tune the phase composition of precipitated CaSO_4 powders in a one-step process at ambient conditions simply by adjusting the water content of the solvent medium – yielding pure anhydrite at

<0.2 wt% H₂O, pure bassanite between 2 and 30 wt% H₂O, and pure gypsum at >50 wt% H₂O – while at intermediate values mixtures with defined compositions are obtained.

12.3.2 *Crystallization of Bassanite and Anhydrite*

Compared to gypsum, relatively little is known about the early stages of the crystallization of bassanite and anhydrite from aqueous solution. Several studies have focused on establishing the temperature and salinity regions where these phases form spontaneously, mainly by characterizing the outcome of direct precipitation experiments (i.e., mixing Ca²⁺- and SO₄²⁻-containing solutions at different conditions) (Cruft and Chao 1970; Ossorio et al. 2014). Although solubility measurements predict anhydrite as the stable phase above 40–60 °C (cf. Fig. 12.2a and Sect. 12.2.2 above), gypsum was always the major product obtained up to 90 °C, while at higher temperatures mainly bassanite was formed (likely due to the kinetic inhibition of anhydrite mentioned above). Interestingly, the temperature for the primary precipitation of bassanite can be significantly lowered by increasing the ionic strength of the reacting solutions, in particular by using highly concentrated electrolyte solutions (Cruft and Chao 1970; Jiang et al. 2013; Ossorio et al. 2014). For example, bassanite is formed already at 80 °C in the presence of 4.5 M NaCl (Ossorio et al. 2014), while a temperature of around 50 °C is sufficient to produce pure hemihydrate from solutions containing >6 M CaCl₂ and small amounts of Na₂SO₄ (Cruft and Chao 1970). This again hints at the importance of hydration effects during the crystallization process, which are likely to change substantially as the activity of water is modulated at high salt contents. Another observation pointing in the same direction is the fact that bassanite forms spontaneously during the evaporation of droplets of CaSO₄ solutions at room temperature (Qian et al. 2012; Shahidzadeh et al., 2015). In those cases, the relative humidity (RH < ~80 %) and the time-dependent availability of water – potentially along with confinement effects during the evaporation process – seem to be the controlling factors for phase selection. Although the conditions needed to induce bassanite formation in purely aqueous systems appear to be fairly well known, so far distinct insight into the details of the nucleation mechanisms and pathways is still missing.

To the best of our knowledge, there is only one published study that reports on the kinetics of direct anhydrite precipitation in aqueous media at temperatures between 100 and 200 °C and at a constant salt content of 1 M NaCl (Fan et al. 2010). Although no precipitation was observed at 118 and 148 °C, induction times could be measured as a function of supersaturation at 178 °C. Based on these results, the authors estimated the effective surface free energy of anhydrite to be 92.9 mJ/m². This value is roughly twice as high as that for gypsum and explains why anhydrite does not readily form in its own thermodynamic stability region (Ossorio et al. 2014). Since the nucleation rate depends strongly (to the power of 3 according to CNT) on the surface free energy of the emerging mineral phase, it is

reasonable that gypsum ($\sim 40 \text{ MJ/m}^2$) and bassanite ($\sim 9 \text{ MJ/m}^2$) (Guan et al. 2010) form much more readily than anhydrite across large parts of the phase diagram (Ossorio et al. 2014). Similar to the case of bassanite, the presence of high concentrations of salt in the reacting solutions can facilitate the formation of anhydrite. This was recently shown by Dixon et al. (2015), who studied the dissolution of jarosite, $(\text{K,Na,H}_3\text{O})\text{Fe}_3(\text{SO}_4)_2(\text{OH})_6$, in saturated CaCl_2 brines under ambient conditions. In their experiments, the release of sulfate and the high concentration of calcium in the medium inevitably led to precipitation of calcium sulfates. Interestingly, the resulting phase composition varied depending on the particular procedure applied, with experiments conducted in a batch reactor (i.e., a closed system) yielding a mixture of gypsum and bassanite, whereas in a flow-through setup the main product was anhydrite. This is the first experimental evidence that anhydrite can spontaneously nucleate in aqueous environments at room temperature (i.e., without organic (co)solvents), confirming the previously predicted stability region of anhydrite in high-salinity brines (Bock 1961; Hardie 1967). Initial nucleation of gypsum and subsequent transformation into anhydrite represent an unlikely scenario under these conditions, due to the slow dehydration rates of gypsum near the predicted anhydrite-gypsum transition temperature ($\sim 18 \text{ }^\circ\text{C}$ at the given salinity) (Hardie 1967). Again, one could argue that water activity and corresponding changes in the hydration of solute precursors are crucial for phase selection in the CaSO_4 system – with very high salt contents leading to anhydrite, much like extremely low water contents caused anhydrite formation in the work of Tritschler et al. (2015b).

12.3.3 *Influence of Additives on Nucleation and Phase Transformation*

Based on numerous studies for a variety of mineral systems, it is a well-established fact that both organic and inorganic additives can have a substantial influence on the outcome of crystallization processes, in some cases already at very low concentrations (e.g., Gebauer et al. 2009). Although this subject has not been frequently addressed for the calcium sulfate system in the past, there are a few interesting observations, which shall be summarized in the following.

Probably the most compelling example is found in biomineralization, where two classes of medusae use bassanite for their gravitational sense (Tienmann et al. 2002; Becker et al. 2005; Boßelmann et al. 2007). The *tour de force* achieved by these organisms is twofold: (I) they induce the nucleation, growth, and stabilization of well-defined macroscopic bassanite crystals at room temperature – something that in the lab can only be realized above $50 \text{ }^\circ\text{C}$ and at extreme high salinity (see Sect. 12.3.2) (Cruft and Chao 1970; Ossorio et al. 2014); (II) they manage to stabilize this highly hygroscopic material in a water-rich environment – usually bassanite transforms immediately into gypsum when put in contact with moisture

(explaining its scarcity on the Earth's surface). At present any conclusive mechanistic insights into how this is achieved are lacking, but it is reasonable to assume that molecules of biological origin (such as proteins, peptides, or polysaccharides) and/or confinement effects may be responsible for this impressive level of control. Support for this hypothesis has been reported by Tartaj et al. (2015), who performed CaSO_4 mineralization in carboxy- and amino-functionalized reverse micelles and observed that strong binding between calcium and carboxylate groups can lead to long-term (up to 5 months) stabilization of nano-bassanite.

Already in 1980, Cody and Hull studied the influence of organic crystallization inhibitors on the precipitation pathway of calcium sulfate close to the gypsum/anhydrite transition temperature (i.e., 60 °C) and at moderate salinity (Cody and Hull 1980). First, they tested the effect of a range of different additives in diffusion-controlled crystallization experiments, where in the absence of any additives only gypsum was formed (over a remarkable period of up to 4 years). The presence of polycarboxylates and phosphate esters changed the picture completely, as anhydrite was the only product detected after 60 days. In a second set of controlled mixing experiments, anhydrite was formed both by direct precipitation from solution and via transformation of initially nucleated gypsum and/or bassanite, again under the influence of the mentioned organic species. The authors proposed that the primary role of the polymeric additives was to inhibit gypsum and bassanite crystallization, rather than accelerating anhydrite nucleation. However, the particular mechanism and the question whether (and under which conditions) the formation of anhydrite involves a precursor remained unresolved. Nevertheless, it seems clear that certain polymers can promote anhydrite crystallization at relatively low temperatures, which is not possible in pure CaSO_4 solutions.

Along with the more recent finding that amorphous calcium sulfate and/or bassanite may precede the formation of gypsum in aqueous solutions at ambient conditions (Wang et al. 2012; Van Driessche et al. 2012; Saha et al. 2012; Jones 2012), the influence of additives on the precipitation pathway and the (meta)stability of the different precursors received further attention. In the cryo-TEM work of Saha et al. (2012), added citrate ions were found to stabilize the initial disordered phase and thus delayed its transformation into gypsum. Wang and Meldrum (2012) performed another study in which CaSO_4 precipitation was carried out in the presence of polyacrylic acid (PAA), polystyrene sulfonate (PSS), sodium triphosphate, and Mg^{2+} ions. In essence, the results suggested that all these additives, except PSS, can retard the transformation of both amorphous calcium sulfate and bassanite to a greater or lesser extent. For instance, 200 $\mu\text{g/mL}$ PAA were found to increase the lifetime of ACS and bassanite particles to a few minutes and more than 3 days, respectively. This effect was also observed by Rabizadeh et al. (2014), who showed that even at lower concentrations (5–20 $\mu\text{g/mL}$) carboxylic acids can change the induction times and stabilize bassanite prior to its transformation to gypsum. In the work of Wang and Meldrum (2012), sodium triphosphate showed similar behavior

at 20 $\mu\text{g/mL}$, while the presence of magnesium (at a $\text{Mg}^{2+}/\text{Ca}^{2+}$ ratio of 2:1) stabilized mainly bassanite (up to 2 days). Although this appears to be a promising concept to control CaSO_4 mineralization, we note that the procedure used in these studies for isolation and analysis of the precursor phases from solution involved quenching in ethanol – a step that has proven to be critical and may affect phase composition or even induce the formation of structures that were actually not present before (Tritschler et al. 2015a, b). A different approach to the stabilization of ACS and bassanite was reported by Nissinen et al. (2014), who dissolved calcium sulfate in *N*-methylmorpholine *N*-oxide (NMMO) along with cellulose at 80 °C and prepared thin films by spin-coating and subsequent hydration. The resulting CaSO_4 phase was determined by the rate of hydration – once more highlighting the key role of water availability in the precipitation process.

12.3.4 Toward a General Model for CaSO_4 Precipitation from Solution

In the previous sections, we have discussed a number of early and more recent studies on the crystallization of calcium sulfate from solution. While at first sight there seems to be quite some disagreement between the various reported observations, closer examination and consideration of the details intrinsic to each work suggest that all the evidence is converging into a unified general picture of CaSO_4 mineralization. In Fig. 12.6 we have sketched out our opinion about the key stages along the pathway from homogeneous solutions to crystalline phases.

In undersaturated solutions, calcium and sulfate occur both as individual ions and ion pairs (Garrels and Christ 1965). Whether they also form larger species, akin to the pre-nucleation clusters suggested for other salt systems, is still unclear and the respective equilibrium constants of ion association remain to be determined. The evidence so far suggests that when supersaturation is established, primary nanosized units are formed by the assembly of multiple ions into rather well-defined elongated entities, the structure of which can be related to any of the possible crystalline phases. These primary units thus represent sort of a universal CaSO_4 proto-structure (see Fig. 12.4). With time and through fluctuations, these primary units begin to aggregate and condense, yielding domains that initially are mostly disordered (possibly corresponding to amorphous calcium sulfate, although this is still debated). These domains consist of the primary units separated by appreciable amounts of solvent. In order to transform into well-ordered sheets of CaSO_4 cores with more (gypsum), less (bassanite), or no (anhydrite) interspersed H_2O layers, the disordered precursors must reorganize by progressive coalescence of the primary species into larger units. During this internal rearrangement, there will be local domains that adopt configurations that are not (yet) fully hydrated and ordered, especially during the early stages of the transformation process. Therefore, the local availability of water and the particular degree of hydration of the precursor units

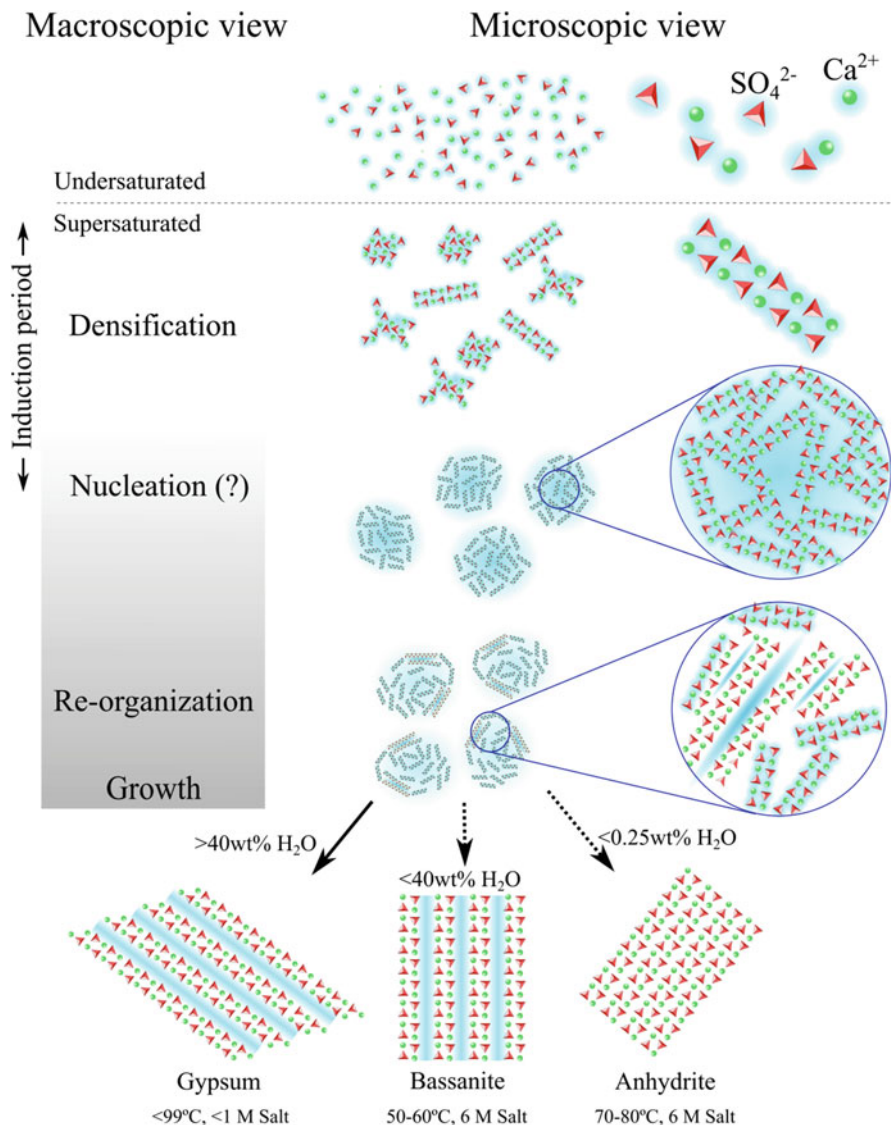


Fig. 12.6 Proposed mechanism for the nucleation and early growth of calcium sulfate from solution. Note that the nature of the formed crystalline phase essentially depends on the availability of water in the medium (respective water contents are quoted) and the hydration of the precursor units, which is further influenced by temperature and salinity (tentative conditions are indicated)

control which crystalline phase is favored under the given conditions. As both of these factors are inherently time-dependent, kinetics are likely to have a strong impact on the final outcome. Once structural rearrangement has afforded an ordered lattice (i.e., the crystalline state has nucleated), growth takes over and rapidly yields

larger particles due to the high concentration of (still disordered) CaSO_4 units in the local microenvironment. Nevertheless, the actual mechanism of growth remains to be clarified.

Based on this precipitation scheme, most of the recent (and older) experimental evidence can be rationalized. Beyond that, this pathway reveals an intriguing strategy to guide the precipitation process in the calcium sulfate system, namely, by controlling the available amount of water or, respectively, by modulating the hydration of the precursor units. Using defined mixtures of organic solvents and water is a viable approach to achieve this, as demonstrated in the work of Tritschler et al. (2015a, b). The importance of kinetics in the process has been exemplified by the experiments of Nissinen et al. (2014), where the differences in the hydration rate in pure water and water/ethanol mixtures proved to determine phase selection. Apart from the use of organic solvents, the hydration of the precursor units can also be influenced in purely aqueous media, namely, by changing salinity and/or temperature. Increasing any of the two parameters is expected to decrease the degree of hydration, as higher temperatures should favor the return of hydration water into the bulk (for entropic reasons) (Paula et al. 1995; Damasceno et al. 2012; Kellermeier et al. 2016), while microscopic osmotic forces should also remove water from the precursors at high salt content (Di Tommaso et al. 2014). This hypothesis is supported by the well-established trend that bassanite replaces gypsum as the primary phase formed at high enough temperatures and/or salinities (cf. Sect. 12.3.2) (Cruft and Chao 1970; Jiang et al. 2013; Ossorio et al. 2014). Moreover, it may explain the kinetic inhibition of anhydrite crystallization observed under various conditions: regardless of any thermodynamic stability fields, it is very difficult to remove enough water from the precursors in an aqueous environment for anhydrite to be able to compete with bassanite and gypsum. Drastically decreasing the availability of water – for example, by working in organic solvents that contain only trace amounts of H_2O (Tritschler et al. 2015b) or by increasing salinity to extreme values (Cruft and Chao 1970) – can change the situation and induce direct anhydrite formation, although the particular precipitation procedure seems to play an important role here as well (Dixon et al. 2015). Finally, it is feasible that additives such as organic polymers (Cody and Hull 1980; Wang and Meldrum 2012) or Mg^{2+} ions (Wang and Meldrum 2012) also act upon the initial process of phase selection and/or the later kinetic stability of nucleated phases by modulating local hydration phenomena. All these hypotheses await confirmation by further studies.

12.4 Outlook

Although significant advances have been made in our understanding of the precipitation of solid phases in the $\text{CaSO}_4\text{--H}_2\text{O}$ system, there is still a considerable dearth of basic information that is crucial for a complete and comprehensive model of nucleation, growth, and transformation of the different CaSO_4 phases. In our opinion, the following key issues should be addressed in future work:

- Unambiguous determination of both bulk and nanoparticle solubilities (and thus relative stabilities) for the different calcium sulfate phases
- Actual measurements of the degree of hydration at different precursor stages under various conditions to verify the role of water in the process of phase selection, along with the influence of additives and other factors like confinement
- Characterization of ion association phenomena in undersaturated solutions with respective equilibrium constants, existence (or not) of CaSO_4 pre-nucleation clusters (i.e., larger species beyond ion pairs), relation of any such clusters to the elongated primary species occurring in supersaturated solutions
- Determination of the actual structure and (meta)stability of the primary species and the driving force triggering their initial aggregation and later crystallization to one or the other CaSO_4 phase
- Identification of the actual nucleation step in the $\text{CaSO}_4\text{-H}_2\text{O}$ system (i.e., the stage where an interface emerges), distinction of the observed structures into solution species (pre-nucleation) and solid particles (post-nucleation)
- More elaborate study of the nucleation pathways of anhydrite and bassanite to confirm, or refute, the hypotheses made above
- Confirming the existence of a truly disordered (ACS) phase and characterizing its properties with respect to parameters like local order, solubility, density, etc.
- Clarifying the role of the observed primary species in the growth of macroscopic calcium sulfate crystals
- Verification of the relevance of the mechanisms described above for CaSO_4 formation under real application conditions (e.g., for the case of construction materials or scaling from hard water)
- Comparison of the precipitation pathways found for calcium sulfate with those of other important sulfate minerals, such as BaSO_4 and SrSO_4

While obviously much is left to be unveiled, the progress made over the past few years promises deeper insights in the near future that will hopefully help to improve existing calcium sulfate-based materials and possibly become integrated into a still larger unified picture of crystallization mechanisms from solution in general.

Acknowledgments The authors thank Dr. Alejandro Fernandez-Martinez (ISTerre, France) and Dr. Luc Nicoleau (BASF) for valuable discussions. TMS and LGB were funded by a Helmholtz Recruiting Initiative Grant to LGB for this work.

References

- Abriel W (1983) Calcium sulfate subhydrate, $\text{CaSO}_4 \cdot 0.8\text{H}_2\text{O}$. *Acta Crystallogr Sect C* 39:956–958
- Ahmed SB, Tlili M, Amor MB, Bacha HB, Eullech B (2004) Calcium sulphate scale prevention in a desalination unit using the SMCEC technique. *Desalination* 167:311–318
- Alimi F, Elfil H, Gadri A (2003) Kinetics of the precipitation of calcium sulfate dihydrate in a desalination unit. *Desalination* 157:9–16
- Allen RD, Kramer H (1953) Occurrence of bassanite in two desert basins in southeastern California. *Am Mineral* 38:1266–1268

- Andreassen JP, Lewis AE (2017) Classical and nonclassical theories of crystal growth. In: Van Driessche AES, Kellermeier M, Benning LG, Gebauer D (eds) *New perspectives on mineral nucleation and growth*, Springer, Cham, pp 137–154
- Apokodje EG (1984) The occurrence of bassanite in some Australian arid-zone soils. *Chem Geol* 47:361–364
- Azimi G, Papangelakis VG (2010) The solubility of gypsum and anhydrite in simulated laterite pressure acid leach solutions up to 250 °C. *Hydrometallurgy* 102:1–13
- Azimi G, Papangelakis VG, Dutrizac JE (2007) Modelling of calcium sulphate solubility in concentrated multi-component sulphate solutions. *Fluid Phase Equilib* 260:300–315
- Becker R, Doring W (1935) Kinetic treatment of grain-formation in super-saturated vapours. *Ann Phys* 24:719–752
- Becker A, Sötje I, Paulmann C, Beckmann F, Donath T, Boese R, Prymak O, Tiemann H, Epple M (2005) Calcium sulphate hemihydrate is the inorganic mineral in statoliths of scyphozoan medusae (Cnidaria). *Dalton Trans* 8:1545–1550
- Birkedal H (2017) Phase transformations in calcium phosphate crystallization. In: Van Driessche AES, Kellermeier M, Benning LG, Gebauer D (eds) *New perspectives on mineral nucleation and growth*, Springer, Cham, pp 199–210
- Block J, Waters OB (1968) The $\text{CaSO}_4\text{-Na}_2\text{SO}_4\text{-NaCl-H}_2\text{O}$ system at 25 to 100 °C. *J Chem Eng Data* 13:336–344
- Blount CW, Dickson FW (1969) The solubility of anhydrite (CaSO_4) in $\text{NaCl-H}_2\text{O}$ from 100 to 450°C and 1 to 1000 bars. *Geochim Cosmochim Acta* 33:227–245
- Blount CW, Dickson FW (1973) Gypsum-anhydrite equilibria in systems $\text{CaSO}_4\text{-H}_2\text{O}$ and $\text{CaSO}_4\text{-NaCl-H}_2\text{O}$. *Am Mineral* 58:323–331
- Boßelmann F, Epple M, Sötje I, Tiemann H (2007) Statoliths of calcium sulfate hemihydrate are used for gravity sensing in rhopalioophoran medusae (Cnidaria). In: Baeuerlein E (ed) *Biom mineralisation: biological aspects and atructure formation*. Wiley-VCH, Weinheim, pp 261–272
- Booth E (1961) On the solubility of anhydrous calcium sulphate and of gypsum in concentrated solutions of sodium chloride at 25 °C. *Can J Chem* 39:1746–1751
- Booth HS, Bidwell RM (1950) Solubilities of salts in water at high temperatures. *J Am Chem Soc* 72:2567–2575
- Boyer-Guillon M (1900) Etude sur la solubilité du sulfate de chaux. Extrait des Annales du Conservatoire des Arts et Metiers, 3^e serie, tome II
- Cameron FK (1901) Solubility of gypsum in aqueous solutions of sodium chloride. *J Phys Chem* 5:556–576
- Chang LLY, Howie RA, Zussman J (1996) *Rock-forming minerals*, Vol. 5B: Non-silicates, longman scientiçc and technical. Harlow, 383 pp
- Charola AE, Pühringer J, Steiger M (2007) Gypsum: a review of its role in the deterioration of building materials. *Environ Geol* 52:339–352
- Christiansen JA, Nielsen AE (1952) The interplay between nucleus formation and crystal growth. *Z Elektrochem* 56:465
- Cody RD, Hull AB (1980) Experimental growth of primary anhydrite at low temperatures and water salinities. *Geology* 8:505–509
- Conley RF, Bundy WM (1958) Mechanism of gypsification. *Geochim Cosmochim Acta* 15:57–72
- Corti HR, Fernandez-Prini R (1983) Thermodynamics of solution of gypsum and anhydrite in water over a wide temperature range. *Can J Chem* 62:484–488
- Cruft EF, Chao PC (1970) Nucleation kinetics of the gypsum-anhydrite system. In: 3rd symposium on salt, northern Ohio geological society proceedings, vol 1, pp 109–118
- Culberson CH, Lathman G, Bates RG (1978) Solubilities and activity coefficients of calcium and strontium sulfate in synthetic seawater at 0.5 and 25 °C. *J Phys Chem* 82:2693–2699
- D’Ans J (1933) *Die Lösungsgleichgewichte der Systeme der Salze ozeanischer Salzablagerungen*. Verlagsgesellschaft für Ackerbau, Berlin, p 5
- D’Ans J (1968) Der Übergangspunkt Gips-Anhydrit. *Kali Steinsalz* 5:109–111

- Damasceno PF, Engel M, Glotzer SC (2012) Crystalline assemblies and densest packings of a family of truncated tetrahedra and the role of directional entropic forces. *ACS Nano* 6:609–614
- De Yoreo JJ, Sommerdijk NAJM, Dove PM (2017) Nucleation pathways in electrolyte solutions. In: Van Driessche AES, Kellermeier M, Benning LG, Gebauer D (eds) *New perspectives on mineral nucleation and growth*, Springer, Cham, pp 1–24
- Delgado-López JM, Guagliardi A (2017) Control over nanocrystalline apatite formation: what can the X-ray total scattering approach tell us. In: Van Driessche AES, Kellermeier M, Benning LG, Gebauer D (eds) *New perspectives on mineral nucleation and growth*, Springer, Cham, pp 211–226
- Demichelis R, Raiteri P, Gale JD (2017) Ab Initio modelling of the structure and properties of crystalline calcium carbonate. In: Van Driessche AES, Kellermeier M, Benning LG, Gebauer D (eds) *New perspectives on mineral nucleation and growth*, Springer, Cham, pp 113–136
- Dey A, Bomans PHH, Müller FA, Will J, Frederik PM, de With G, Sommerdijk NAJM (2010) The role of prenucleation clusters in surface-induced calcium phosphate crystallization. *Nat Mater* 9:1010–1014
- Dickson FW, Blount CW, Tunell G (1963) Use of hydrothermal solution equipment to determine the solubility of anhydrite in water from 100 °C to 275 °C and from 1 bar to 1000 bars pressure. *Am J Sci* 261:61–78
- Di Tommaso D, Ruiz-Agudo E, de Leeuw NH, Putnis A, Putnis CV (2014) Modelling the effects of salt solutions on the hydration of calcium ions. *Phys Chem Chem Phys* 16:7772–7785
- Dixon EM, Elwood Madden AS, Hausrath E, Elwood Madden ME (2015) Assessing hydrodynamic effects on jarosite dissolution rates, reaction products, and preservation on Mars. *J Geophys Res* 120:625–642
- Dongan AU, Dogan M, Chan DCN, Wurster DE (2005) Bassanite from *Salvadora persica*: a new evaporitic biomineral. *Carbonates Evaporites* 20:2–7
- Droeze H (1877) Solubility of gypsum in water and in saline solutions. *Bericht d. deutsch. chem. Ges. in Berlin*. 10:330–343
- Fan C, Kan AT, Fu G, Tomson MB (2010) Quantitative evaluation of calcium sulfate precipitation kinetics in the presence and absence of scale inhibitors. *SPE J* 15:977–988
- Falini G, Fermani S (2017) Nucleation and growth from a biomineralization perspective. In: Van Driessche AES, Kellermeier M, Benning LG, Gebauer D (eds) *New perspectives on mineral nucleation and growth*, Springer, Cham, pp 185–198
- Fernandez-Martinez A, Lopez-Martinez H, Wang D (2017) Structural characteristics and the occurrence of polyamorphism in amorphous calcium carbonate. In: Van Driessche AES, Kellermeier M, Benning LG, Gebauer D (eds) *New perspectives on mineral nucleation and growth*, Springer, Cham, pp 77–92
- Freyer D, Voigt W (2003) Crystallization and phase stability of CaSO₄ and CaSO₄-based salts. *Monatsh Chem* 134:693–719
- Garcia-Ruiz JM, Villasuso R, Ayora C, Canals A, Otalora F (2007) Formation of natural gypsum megacrystals in Naica, Mexico. *Geology* 35:327–330
- Garrels RM, Christ CL (1965) *Solutions, minerals and equilibria*. Harper and Row, New York, 450 p
- Gebauer D, Völkel A, Cölfen H (2008) Stable prenucleation calcium carbonate clusters. *Science* 322:1819
- Gebauer D, Cölfen H, Verch A, Antonietti M (2009) The multiple roles of additives in CaCO₃ crystallization: a quantitative case study. *Adv Mater* 21:435
- Guan B, Yang L, Wu Z (2010) Effect of Mg²⁺ ions on the nucleation kinetics of calcium sulfate in concentrated calcium chloride solutions. *Ind Eng Chem Res* 49:5569–5574
- Hall RE, Robb JA, Coleman CE (1926) The solubility of calcium sulfate at boiler-water temperatures. *J Am Chem Soc* 48:927–938
- Hamad S el D (1985) The transition temperature of gypsum and anhydrite. *Sudan J Sci* 1:48
- Hamdona SK, Nessim RB, Hamza SM (1993) Spontaneous precipitation of calcium sulfate dihydrate in the presence of some metal ions. *Desalination* 94:69–80

- Hardie LA (1967) The gypsum-anhydrite equilibrium at one atmosphere pressure. *Am Mineral* 52:171–200
- He S, Oddo JE, Tomson MB (1994) The nucleation kinetics of calcium sulfate dihydrate in NaCl solutions up to 6 m and 90°C. *J Colloid Interface Sci* 162:297–303
- Hill AE (1937) The transition temperature of gypsum to anhydrite. *J Am Chem Soc* 59:2242–2244
- Hill AE, Wills JH (1938) Ternary systems. XXIV. Calcium sulfate, sodium sulfate and water. *J Am Chem Soc* 60:1647–1655
- Hulett GA, Allen LE (1902) The solubility of gypsum. *J Am Chem Soc* 24:667–679
- Innorta G, Rabbi E, Tomadin L (1980) The gypsum-anhydrite equilibrium by solubility measurements. *Geochim Cosmochim Acta* 44:1931–1936
- Jiang G, Mao J, Fu H, Zhou X, Guan B (2013) Insight into metastable lifetime of a-calcium sulfate hemihydrate in CaCl₂ solution. *J Am Ceram Soc* 96:3265–3271
- Jones F (2012) Infrared investigation of barite and gypsum crystallization: evidence for an amorphous to crystalline transition. *CrystEngComm* 14:8374–8381
- Kashchiev D (2000) Nucleation: basic theory with applications. Butterworth-Heinemann, Oxford
- Kellermeier M, Picker A, Kempter A, Cölfen H, Gebauer D (2014) A straightforward treatment of activity in aqueous CaCO₃ solutions and the consequences for nucleation theory. *Adv Mater* 26:752
- Kellermeier M, Raiteri P, Berg JK, Kempter A, Gale JD, Gebauer D (2016) Entropy drives calcium carbonate ion association. *Chem Phys Chem*. doi:10.1002/cphc.201600653
- Kelley KK, Southard JC, Anderson CT (1941) Thermodynamic properties of gypsum and its dehydration products, vol 625, US bureau mines technical paper. U.S. G.P.O, Washington, DC
- Klepetsanis PG, Koutsoukos PG (1989) Precipitation of calcium sulfate dihydrate at constant calcium activity. *J Cryst Growth* 98:480
- Klepetsanis PG, Dalas E, Koutsoukos PG (1999) Role of temperature in the spontaneous precipitation of calcium sulfate dihydrate. *Langmuir* 15:1534–1540
- Knacke O, Gans W (1977) The thermodynamics of the system CaSO₄-H₂O. *Z Phys Chem NF* 104:41–48
- Kontrec J, Kralj D, Breèeviaè L (2002) Transformation of anhydrous calcium sulphate into calcium sulphate dihydrate in aqueous solutions. *J Cryst Growth* 240:203–211
- Lager GA, Armbruster T, Rotella FJ, Jorgensen JD, Hinks DG (1984) A crystallographic study of the low-temperature dehydration products of gypsum, CaSO₄·2H₂O: hemihydrate CaSO₄·0.5H₂O, and γ-CaSO₄. *Am Mineral* 69:910–918
- Lancia A, Musmarra D, Prisciandaro M (1999) Measuring induction period for calcium sulfate dihydrate precipitation. *AIChE J* 45:390–397
- Langevin Y, Poulet F, Bibring JP, Gondet B (2005) Sulfates in the north polar region of Mars detected by OMEGA/Mars express. *Science* 307:1584–1586
- Lewry AJ, Williamson J (1994) The hydration of calcium sulphate hemihydrate. *J Mat Sci* 29:5279–5284
- Ling Z, Wang A (2015) Spatial distributions of secondary minerals in the Martian meteorite MIL 03346.168 determined by Raman spectroscopic imaging. *J Geophys Res*. doi:10.1002/2015JE004805
- Liu ST, Nancollas GH (1973) Linear crystallization and induction-period studies of the growth of calcium sulphate dihydrate crystals. *J Colloid Interface Sci* 44:422
- Lu H, Kan A, Zhang P, Yu J, Fan C, Work S, Tomson MB (2012) Phase stability and inhibition of calcium sulfate in the system NaCl/Monoethylene Glycol/H₂O. *SPE J* 17:187–198
- Madgin WM, Swayles DA (1956) Solubilities in the system CaSO₄-NaCl-H₂O at 25° and 35° C. *J Appl Chem* 6:482–487
- Marignac C (1874) Ueber die Löslichkeit des schwefelsauren kalkes in wasser. *Z Anal Chem* 13: 57–59
- Marshall WL, Slusher R (1966) Thermodynamics of Calcium Sulfate Dihydrate in Aqueous sodium chloride solutions, 0– 110°. *J Phys Chem* 70:4015–4027

- Marshall WL, Slusher R, Jones EV (1964) Aqueous systems at high temperature. XIV. Solubility and thermodynamic relationships for CaSO_4 in $\text{NaCl-H}_2\text{O}$ solutions from 40 °C to 200 °C, 0 to 4 molal NaCl . *J Chem Eng Data* 9:187
- Melcher AC (1910) The solubility of silver chloride, barium sulphate, and calcium sulphate at high temperatures. *J Am Chem Soc* 32:50–66
- Mi B, Elimelech M (2010) Gypsum scaling and cleaning in forward osmosis: measurements and mechanisms. *Environ Sci Technol* 44:2022–2028
- Momma K, Izumi F (2011) VESTA 3 for three-dimensional visualization of crystal, volumetric and morphology data. *J Appl Crystallogr* 44:1272–1276
- Monnin C (1990) The influence of pressure on the activity-coefficients of the solutes and on the solubility of minerals in the system $\text{Na-Ca-Cl-SO}_4\text{-H}_2\text{O}$ to 200°C and 1 kbar, and to high NaCl concentration. *Geochim Cosmochim Acta* 54:3265–3282
- Navrotsky A (2004) Energetic clues to pathways to biomineralization: precursors, clusters, and nanoparticles. *Proc Natl Acad Sci U S A* 101:12096–12101
- Neville A (2004) The confused world of sulphate attack on concrete. *Cem Concr Res* 34:1275–1296
- Nielsen AE (1964) Kinetics of precipitation. Pergamon Press, Oxford
- Nissinen T, Li M, Davis SA, Mann S (2014) In situ precipitation of amorphous and crystalline calcium sulphates in cellulose thin films. *CrystEngComm* 16:3843–3847
- Osinski GR, Spray JG (2003) Impact-generated carbonate melts: evidence from the Houghton structure, Canada. *Earth Planet Sci Lett* 194:17–29
- Ossorio M, Van Driessche AES, Pérez P, García-Ruiz JM (2014) The gypsum-anhydrite paradox revisited. *Chem Geol* 386:16–21
- Packer A (1971) The precipitation of calcium sulphate dihydrate from aqueous solution induction period, crystal numbers and final size. *J Cryst Growth* 21:191
- Parkhurst DL, Appelo CAJ (1999) User's guide to PHREEQC (version 2). A computer program for speciation, batch-reaction, one-dimensional transport, and inverse geochemical calculations. *Water Resour Invest Rep US Geol Surv* 99(4259):4312
- Partridge E, White AH (1929) The solubility of calcium sulfate from 0 to 200°C. *J Am Chem Soc* 51:360–370
- Paula S, Süss W, Tuchtenhagen J, Blume A (1995) Thermodynamics of micelle formation as a function of temperature: a high sensitivity titration calorimetry study. *J Phys Chem* 99:11742–11751
- Peckmann J, Goedert JL, Heinrichs T, Hoefs J, Reitner J (2003) The late eocene 'Whiskey Creek' methane-seep deposit (western Washington State)—part II: petrology, stable isotopes, and biogeochemistry. *Facies* 48:241–254
- Penn RL, Li D, Soltis JA (2017) A perspective on the particle-based crystal growth of ferric oxides, oxyhydroxides, and hydrous oxides. In: Van Driessche AES, Kellermeier M, Benning LG, Gebauer D (eds) *New perspectives on mineral nucleation and growth*, Springer, Cham, pp 257–274
- Poggiale M (1843) Memoire sur la solubilité des sels dans l'eau. *Ann Chim Phys* 3:463–478
- Posnjak E (1938) The system $\text{CaSO}_4\text{-H}_2\text{O}$. *Am J Sci* 35:247–272
- Power WH, Fabuss BM, Satterfield CN (1964) Transient solubilities in the calcium sulfate-water system. *J Chem Eng Data* 9:437
- Power WH, Fabuss BM, Satterfield CN (1966) Transient solute concentrations and phase changes of calcium sulfate in aqueous sodium chloride. *J Chem Eng Data* 11:149–154
- Prisciandaro M, Lancia A, Musmarra D (2001a) Calcium sulphate dihydrate nucleation in the presence of calcium and sodium chloride salts. *Ind Eng Chem Res* 40:2335–2339
- Prisciandaro M, Lancia A, Musmarra D (2001b) Gypsum nucleation into sodium chloride solutions. *AIChE J* 47:929–934
- Prisciandaro M, Lancia A, Musmarra D (2003) The retarding effect of citric acid on calcium sulfate nucleation kinetics. *Ind Eng Chem Res* 42:6647–6652
- Qian Z, Wang F, Zheng Y, Yu J, Zhang Y (2012) Crystallization kinetics of sea-salt aerosols studied by high-speed photography. *Chin Sci Bull* 57:591–594

- Rabizadeh T, Peacock CL, Benning LG (2014) Carboxylic acids: effective inhibitors for calcium sulfate precipitation. *Mineral Mag* 78:1465–1472
- Raju KUG, Atkinson G (1990) The thermodynamics of “scale” mineral solubilities. 3. Calcium sulfate in aqueous NaCl. *J Chem Eng Data* 35:361
- Rao A, Cölfen H (2017) Mineralization schemes in the living world: mesocrystals. In: Van Driessche AES, Kellermeier M, Benning LG, Gebauer D (eds) *New perspectives on mineral nucleation and growth*, Springer, Cham, pp 155–184
- Rashad MM, Mahmoud MHH, Ibrahim IA, Abdel-Aal EA (2004) Crystallization of calcium sulfate dihydrate under simulated conditions of phosphoric acid production in the presence of aluminum and magnesium ions. *J Cryst Growth* 267:372–379
- Raupenstrauch GA (1885) Über die Bestimmung der Löslichkeit einiger Salze in Wasser bei verschiedenen Temperaturen. *Monatsh Chem* 6:563–591
- Reichel V, Faivre D (2017) Magnetite nucleation and growth. In: Van Driessche AES, Kellermeier M, Benning LG, Gebauer D (eds) *New perspectives on mineral nucleation and growth*, Springer, Cham, pp 275–292
- Roller PS (1931) Chemical activity and particle size. The rate of solution of anhydrite below 70 microns. *J Phys Chem* 35:1132–1142
- Rodríguez-Blanco JG, Sand KK, Benning LG (2017) ACC and vaterite as intermediates in the solution-based crystallization of CaCO_3 . In: Van Driessche AES, Kellermeier M, Benning LG, Gebauer D (eds) *New perspectives on mineral nucleation and growth*, Springer, Cham, pp 93–112
- Rouchy JM, Monty C (2000) Gypsum microbial sediments: neogene and modern examples. In: Riding RE, Awramik SM (eds) *Microbial sediments*. Springer, Berlin, pp 209–216
- Ryan WBF (2009) Decoding the Mediterranean salinity crisis. *Sedimentology* 56:95–136
- Saha A, Lee J, Pancera SM, Bräuer MF, Kemper A, Tripathi A, Bose A (2012) New insights into the transformation of calcium sulphate hemihydrate to gypsum using time-resolved cryogenic transmission electron microscopy. *Langmuir* 28:11182–11187
- Satava V (1970) Ist α - oder β -gips besser. *Sprechsaal Keramik, Glas*, Email 103:792–798
- Schierholtz OJ (1958) The crystallization of calcium sulphate dihydrate. *Can J Chem* 36:1057–1063
- Shahidzadeh N, Schut MFL, Desarnaud J, Prat M, Bonn D (2015) Salt stains from evaporating droplets. *Sci Rep* 5:10335
- Sharpe R, Cork G (2006) Gypsum and anhydrite. In: Kogel JE, Kogel JE et al (eds) *Industrial minerals & rocks*. Society for Mining, Metallurgy, and Exploration, Inc, Littleton, pp 519–540
- Singh NB, Middendorf B (2008) Calcium sulphate hemihydrate hydration leading to gypsum crystallization. *Prog Cryst Growth Charact Mater* 53:57–77
- Smith BR, Sweett F (1971) The crystallization of calcium sulfate dihydrate. *J Colloid Interface Sci* 37:612–618
- Stawski T, Van Driessche AES, Ossorio M, Rodríguez-Blanco JD, Besselink R, Benning LG (2016) Formation of calcium sulfate through the aggregation of sub-3 nanometre primary species. *Nat Comm* 7:10177
- Tartaj P, Morales J, Fernandez-Diaz L (2015) CaSO_4 mineralization in carboxy- and amino-functionalized reverse micelles unravels shape-dependent transformations and long-term stabilization pathways for poorly hydrated nanophases (bassanite). *Cryst Growth Des* 15:2809–2816
- Tiemann H, Sötje I, Jarms G, Paulmann C, Epple M, Hasse B (2002) Calcium sulphate hemihydrate in statoliths of deep-sea medusae. *J Chem Soc Dalton Trans* 7:1266–1268
- Tilden WA, Shenstone WA (1984) On the solubility of salts in water at high temperatures. *Philos Trans R Soc* 175A:31
- Tobler DJ, Stawski TM, and Benning LG (2017) Silica and alumina nanophases: natural processes and industrial applications. In: Van Driessche AES, Kellermeier M, Benning LG, Gebauer D (eds) *New perspectives on mineral nucleation and growth*, Springer, Cham, pp 293–316

- Tritschler U, Van Driessche AE, Kempter A, Kellermeier M, Cölfen H (2015a) Controlling the selective formation of calcium sulfate polymorphs at room temperature. *Angew Chem Int Ed* 54:4083–4086
- Tritschler U, Kellermeier M, Debus C, Kempter A, Coelfen H (2015b) A simple strategy for the synthesis of well-defined bassanite nanorods. *CrystEngComm* 17:3772–3776
- Van Driessche AES, Garcia-Ruiz JM, Tsukamoto K, Patino-Lopez LD, Satoh H (2011) Ultraslow growth rates of giant gypsum crystals. *Proc Natl Acad Sci U S A* 108:15721–15726
- Van Driessche AES, Benning LG, Rodriguez-Blanco JD, Ossorio M, Bots P, García-Ruiz JM (2012) The role and implications of bassanite as a stable precursor phase to gypsum precipitation. *Science* 336:69–72
- Van't Hoff JH, Armstrong EF, Hinrichsen W, Weigert F, Just G (1903) Gips und anhydrit. *Z Phys Chem* 45:257
- Wang YW, Meldrum FC (2012) Additives stabilize calcium sulfate hemihydrate (bassanite) in solution. *J Mater Chem* 22:22055–22062
- Wang YW, Kim YY, Christenson HK, Meldrum FC (2012) A new precipitation pathway for calcium sulfate dihydrate (gypsum) via amorphous and hemihydrate intermediates. *Chem Commun* 48:504–506
- Warren JK (2006) *Evaporites: sediments, resources and hydrocarbons*. Springer, Berlin
- Weiss H, Bräu MF (2009) How much water does calcined gypsum contain? *Angew Chem Int Ed* 48:3520–3524
- Wolf SE, Gower LB (2017) Challenges and perspectives of the polymer-induced liquid-precursor process: the pathway from liquid-condensed mineral precursors to mesocrystalline products. In: Van Driessche AES, Kellermeier M, Benning LG, Gebauer D (eds) *New perspectives on mineral nucleation and growth*, Springer, Cham, pp 43–76
- Wray JJ, Squyres SW, Roach LH, Bishop JL, Mustard JF, Dobreá NEZ (2010) Identification of the Ca-sulfate bassanite in Mawrth Vallis, Mars. *Icarus* 209:416–421
- Yang L-X, Meng Y-F, Yin P, Yang Y-X, Tang Y-Y, Qin L-F (2011) Shape control synthesis of low-dimensional calcium sulfate. *Bull Mater Sci* 34:233–237
- Zen E (1965) Solubility measurements in the system $\text{CaSO}_4\text{--NaCl--H}_2\text{O}$ at 35° 50° and 70°C and one atmosphere pressure. *J Petrol* 6:124–164
- Zhang H, Banfield JF (2012) Energy calculations predict nanoparticle attachment orientations and asymmetric crystal formation. *J Phys Chem Lett* 3:2882–2886